

Alkane activation on crystalline metal oxide surfaces

Cite this: DOI: 10.1039/c3cs60420a

 Jason F. Weaver,^{*a} Can Hakanoglu,^a Abbin Antony^a and Aravind Asthagiri^b

Advances in the fundamental understanding of alkane activation on oxide surfaces are essential for developing new catalysts that efficiently and selectively promote chemical transformations of alkanes. In this tutorial review, we discuss the current understanding of alkane activation on crystalline metal oxide surfaces, and focus mainly on summarizing our findings on alkane adsorption and C–H bond cleavage on the PdO(101) surface as determined from model ultrahigh vacuum experiments and theoretical calculations. These studies show that alkanes form strongly-bound σ -complexes on PdO(101) by datively bonding with coordinatively-unsaturated Pd atoms and that these molecularly adsorbed species serve as precursors for C–H bond activation on the oxide surface. In addition to discussing the binding and properties of alkane σ -complexes on PdO(101), we also summarize recent advances in kinetic models to predict alkane dissociation rates on solid surfaces. Lastly, we highlight computations which predict that the formation and facile C–H bond activation of alkane σ -complexes also occurs on RuO₂ and IrO₂ surfaces.

Received 18th November 2013

DOI: 10.1039/c3cs60420a

www.rsc.org/csr

Key learning points

- (1) Alkanes form strongly bound σ -complexes on PdO(101) by datively bonding with coordinatively-unsaturated Pd atoms.
- (2) Adsorbed alkane σ -complexes serve as precursors for C–H bond activation on PdO(101).
- (3) The dispersion-corrected DFT-D3 method accurately reproduces alkane binding energies and the energy barrier for propane C–H bond cleavage on PdO(101).
- (4) Entropic contributions have a significant influence on the kinetics of alkane activation on solid surfaces and can be accurately reproduced using appropriate models for the kinetic prefactors that incorporate weakly-hindered modes of the adsorbed species.
- (5) The formation and facile C–H bond activation of adsorbed alkane σ -complexes is predicted to occur on RuO₂ and IrO₂ surfaces and may be a general property of late transition-metal oxide surfaces which expose coordinatively-unsaturated metal and oxygen atom pairs.

1. Introduction

Alkane activation on metal oxide surfaces is a critical step in the catalytic processing of alkanes in applications such as the catalytic combustion of natural gas, exhaust gas remediation and the selective oxidation of alkanes to value-added products. Advances in alkane catalysis are important for realizing technologies that more effectively utilize hydrocarbon resources and would indeed have significant economic and environmental benefits. Despite the importance of catalytic applications with alkanes, relatively few studies of alkane activation on well-defined oxide surfaces have been reported. Because alkanes

interact weakly with many oxides, investigating alkane activation on such surfaces is challenging in typical experiments conducted under ultrahigh vacuum (UHV) conditions. Palladium oxide (PdO) appears to be an exceptional case as recent studies demonstrate that PdO(101) thin films are highly active toward alkanes and readily promote the activation and oxidation of propane and higher *n*-alkanes under UHV conditions.^{1–5} These observations are consistent with reports that PdO formation is responsible for the exceptional activity of high surface-area Pd catalysts in applications of the catalytic combustion of methane under oxygen-rich conditions.⁶ Recent *in situ* investigations have also shown that the PdO(101) facet develops preferentially during the oxidation of Pd(100)^{7,8} and that PdO(101) formation coincides with increased rates of methane oxidation during reaction at millibar pressures.⁹ More generally, experimental and computational investigations with well-defined PdO(101) surfaces have provided a new

^a Department of Chemical Engineering, University of Florida, Gainesville, FL 32611, USA. E-mail: weaver@che.ufl.edu; Fax: +1 352-392-9513; Tel: +1 352-392-0869

^b William G. Lowrie Department of Chemical & Biomolecular Engineering, The Ohio State University, Columbus, OH 43210, USA

1 understanding of alkane activation on oxide surfaces that may
have broad implications for alkane catalysis.

2 In this review, we discuss the current state of understanding
3 of alkane adsorption and activation on well-defined oxide sur-
4 faces as revealed by UHV experiments and quantum chemical
5 calculations based on density functional theory (DFT). We focus
6 the article on the interactions of alkanes with PdO(101) since
7 this system has been studied extensively in recent years and is
8 the only example in which alkane activation on a crystalline
9 oxide surface has been investigated in detail both experimentally
10 and computationally. These studies show that alkane C–H bond
11 activation occurs on PdO(101) by a precursor-mediated mecha-
12 nism wherein a molecularly-adsorbed state serves as the pre-
13 cursor to initial dissociation. A particularly significant finding is
14 that the molecular precursor to dissociation corresponds to
15 adsorbed alkane σ -complexes that form through dative bonding
interactions between alkane molecules and coordinatively

16 unsaturated (cus) Pd atoms at the PdO(101) surface. Alkane
17 σ -complexes represent a type of coordination compound that
18 is well known in organometallic chemistry and thought to serve
19 as a key intermediate in alkane activation by various transition
20 metal compounds;^{10–13} however, experimental evidence for the
21 formation of adsorbed alkane σ -complexes has only been
22 reported for the PdO(101) surface. In addition to discussing
23 the binding and activation of alkane σ -complexes on PdO(101),
24 we also summarize recent kinetic modeling of alkane dissocia-
25 tion on PdO(101). Lastly, we report results which demonstrate
26 that the formation and facile C–H bond activation of alkane
27 σ -complexes occurs on late transition-metal oxide surfaces other
28 than PdO(101). The prediction that alkane activation is facile on
29 several late transition-metal oxides is quite interesting because it
30 suggests the possibility of generating oxide surfaces that exhibit
31 both high activity and selectivity for transforming alkanes to
32 value-added products.



Jason F. Weaver

33 *Jason F. Weaver earned a PhD
34 degree from Stanford University
in 1998, working with Robert
35 Madix to investigate alkane
adsorption on transition metal
surfaces using molecular beam
scattering techniques and
molecular simulations. He
joined the faculty at the
University of Florida in 1999,
where he is currently the
Charles Stokes Professor of
Chemical Engineering and a
Professor of Chemistry by*

*courtesy. Prof. Weaver's research has focused on the growth and
surface chemical properties of Pt and Pd oxide films, and combines
UHV surface analysis methods and molecular simulations. He is
also studying the surface chemistry of rare earth oxides.*



Can Hakanoglu

36 *Can Hakanoglu earned his
37 Bachelor of Science degree from
the chemical engineering
department of the Istanbul
38 Technical University in 2006. He
joined the chemical engineering
master's program at the
University of Florida in 2007.
He began working with Dr Jason
Weaver in 2008 and earned his
39 PhD degree from the chemical
engineering department of the
University of Florida in 2013.*

*His research mainly focused on
investigating the kinetics of alkane adsorption and reaction on Pd
oxide surfaces using ultrahigh vacuum techniques. He joined the
Intel Corp. Logic Technology Development Group in 2013 where he
currently works as a process engineer.*



Abbin Antony

41 *Abbin Antony earned his doctoral
42 degree in chemical engineering
from University of Florida in
43 2013, where he worked with
Jason F. Weaver and Aravind R.
44 Asthagiri to explore different late-
transition metal oxide surfaces
and investigate the chemical
activity of various molecular
species on these surfaces
employing ab initio quantum
mechanical techniques. He is
45 currently working as a plasma/
dry etch process development
engineer at Intel Corporation.*



Aravind Asthagiri

46 *Dr Aravind Asthagiri obtained his
47 PhD in Chemical Engineering
from Carnegie Mellon University
(2003). In his doctoral research
with Professor David Sholl, he
48 examined the enantiospecificity
of chiral metal surfaces and the
growth of thin metal films on
metal oxides. From 2005–2010
49 he was an assistant professor at
the University of Florida before
joining The Ohio State University
in the fall of 2010 as an associate
50 professor. His research involves*

*the application of atomistic simulations to examine and rationally
design novel materials, with a focus on energy-related applications.*

1.1. Mechanisms for alkane activation on solid surfaces

The initial dissociative chemisorption of an alkane on a solid surface can occur by two general mechanisms, namely, a direct mechanism and a precursor-mediated mechanism.¹⁴ In the direct mechanism, the alkane molecule dissociates during its initial collision with the surface, rather than adsorbing into a molecular state. Direct dissociation is typically activated relative to the energy level of a gas-phase alkane molecule, and the probability for direct dissociation thus increases strongly with increases in the gas temperature and, to a lesser extent, the surface temperature. In the precursor-mediated mechanism, the alkane first adsorbs intact on the surface and the resulting molecularly adsorbed state then serves as a precursor for dissociation. The probability for precursor-mediated dissociation is determined by a kinetic competition between desorption and dissociation of the molecular precursor, and typically exhibits a strong dependence on the surface temperature. The dominance of the direct *vs.* precursor-mediated mechanisms depends on the properties of the molecule–surface system as well as the reaction conditions. Consideration of the main features of the potential energy surface governing an alkane–surface interaction is useful for clarifying the factors which determine the predominant dissociation mechanism.

Fig. 1 shows a representative energy pathway for an alkane–surface interaction which results in alkane dissociation on the surface. This pathway may be considered as a one-dimensional cut through the multi-dimensional potential energy surface, and represents the minimum energy pathway to dissociative chemisorption of an alkane. The zero of energy is taken as the energy of the gaseous alkane molecule at infinite separation from the surface and at rest. The energy pathway features an initial minimum that corresponds to the molecularly adsorbed alkane and a deeper well for the dissociated products, represented as adsorbed R and H species where R depicts an alkyl group. The binding energy of the molecular species has a value of E_d relative to the gas-phase zero where E_d is also

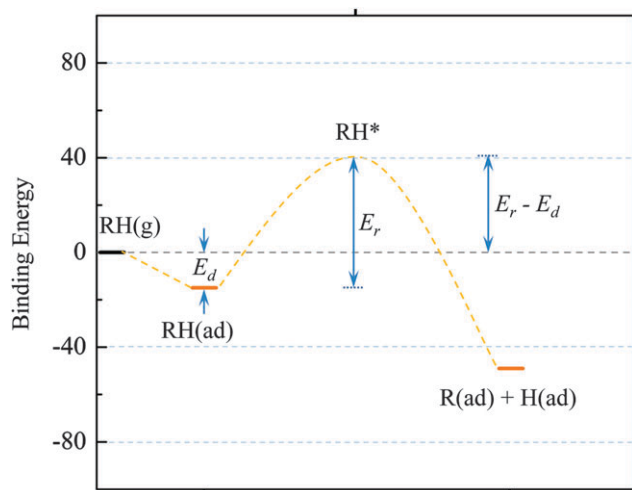


Fig. 1 Schematic energy diagram for the molecular and dissociative chemisorption of an alkane (RH) on a solid surface.

approximately equal to the activation energy for molecular desorption ($d = \text{“desorption”}$). An energy barrier separates the molecularly and dissociatively adsorbed products and has a magnitude of E_r relative to the minimum energy of the molecularly-adsorbed state ($r = \text{“reaction”}$). The so-called apparent barrier for dissociative chemisorption is measured from the gas-phase energy level and has a value of $E_r - E_d$. Fig. 1 shows a case in which the apparent barrier is positive, which means that dissociation is activated relative to the gas-phase energy level. In some cases, however, the barrier lies below the gas-phase level and dissociation is facile.

Direct dissociation can occur in an alkane–surface collision if sufficient energy is channeled into the reaction coordinate to allow the molecule to directly surmount the activation barrier. Direct dissociation tends to become the dominant dissociation mechanism at high reaction temperatures, and may be the only mechanism that is important if the barriers for C–H bond cleavage are large. Precursor-mediated dissociation makes a significant contribution when low energy pathways for dissociation are available and accessible to the molecularly-adsorbed species. The nature of the molecularly adsorbed state plays a central role in determining the importance of the precursor-mediated *vs.* direct pathways. For example, a physically adsorbed methane molecule on an oxide surface has a binding energy of only about 10 to 15 kJ mol⁻¹,^{14–16} while the barriers for alkane C–H bond cleavage on oxides span a wider range, typically between 50 and 150 kJ mol⁻¹.^{5,17,18} For this range of values, the dissociation probability of physisorbed methane will be very small, and the direct mechanism will tend to dominate over the precursor-mediated mechanism. Indeed, methane experiences only weak dispersion interactions with many oxides, such as alkaline earth oxides and rare earth oxides, and direct dissociation appears to be the main mechanism for methane activation in these cases.¹⁸ In contrast, relatively strong molecule–surface dative interactions promote the formation and C–H bond activation of alkane σ -complexes on late transition metal oxide surfaces, causing the precursor-mediated mechanism for alkane dissociation to dominate for this class of oxides.⁵

2. Physical adsorption of alkanes on oxide surfaces

Despite the importance of metal oxides in the catalytic processing of alkanes, only a few investigations of the molecular adsorption of alkanes on well-defined oxide surfaces have been reported. Tait *et al.*^{15,16,19} have reported a thorough investigation of the desorption kinetics of a series of *n*-alkanes physisorbed on MgO(100), a graphitic C(0001) surface and Pt(111). These investigators analyzed temperature programmed desorption (TPD) spectra using a method (inversion-optimization) which allows accurate determination of both the activation energy and kinetic pre-factor for desorption. Their analysis shows that the desorption activation energies increase linearly with increasing chain length for *n*-alkane desorption from each of the surfaces

investigated, and that plots of E_d vs. N exhibit a small y -intercept of only a few kJ mol^{-1} . A particularly significant finding from this work is that the pre-factors for n -alkane desorption increase significantly with increasing chain length, due to increasing gains in the translational and rotational entropy when larger alkanes desorb, and that accounting for this change is necessary for accurately estimating the desorption activation energies.

The explanation for the linear E_d vs. N relationship is that the n -alkanes adopt a flat-lying geometry on these surfaces and that each CH_n group makes a similar, additive contribution to the total binding energy. For the surfaces studied by Tait *et al.*,¹⁹ n -alkane adsorption occurs almost entirely through molecule-surface dispersion interactions (*i.e.*, physisorption). The data reported by Tait *et al.* also show that n -alkanes bind more weakly on $\text{MgO}(100)$ than on $\text{C}(0001)$ and $\text{Pt}(111)$, with the differences in binding energy increasing with chain length. For the C_1 through C_6 n -alkanes, the desorption energies increase from about 12 to 46 kJ mol^{-1} on $\text{MgO}(100)$ and from about 15 to 80 kJ mol^{-1} on $\text{Pt}(111)$.¹⁹ Consistent with the findings of Tait *et al.*,¹⁹ higher binding energies are expected for physisorbed alkanes on a metal vs. an oxide surface since the higher electric polarizability of the metal should strengthen the molecule-surface dispersion interactions.

The molecular adsorption of alkanes has also been investigated on oxides other than $\text{MgO}(100)$. For example, an investigation by Slayton *et al.*²⁰ demonstrates that molecular n -butane, n -hexane and n -octane bind relatively weakly on an $\text{Al}_2\text{O}_3(0001)$ surface, with binding energies similar to that reported for alkanes on $\text{MgO}(100)$. Chakradhar *et al.*²¹ have investigated alkane desorption from a $\text{CaO}(100)$ surface and observe broad desorption features spanning a range from ~ 100 K to at least 300 K, which is indicative of a wide variety of binding sites and/or molecular configurations. The lower temperature desorption features observed in the $\text{CaO}(100)$ study lie in a similar temperature range as those observed in alkane TPD spectra obtained from $\text{MgO}(100)$, while the high temperature features indicate the presence of surface sites that bind the alkanes strongly. As noted by the authors, the strongly-bound alkanes may have originated from surface defect sites as the $\text{CaO}(100)$ samples employed in the work of Chakradhar *et al.*²¹ had high defect densities.

3. Alkane adsorption and activation on $\text{PdO}(101)$

3.1. Structure of the $\text{PdO}(101)$ surface

Experimentally, $\text{PdO}(101)$ surfaces have been generated as thin films by oxidizing $\text{Pd}(111)$ using O-atom beams in UHV under conditions discussed previously.^{22–25} The $\text{PdO}(101)$ thin films are stoichiometrically-terminated, contain between 3 and 4 ML of oxygen atoms and are 10 to 15 Å thick. A model representation of the stoichiometric $\text{PdO}(101)$ surface is shown in Fig. 2. Bulk crystalline PdO has a tetragonal unit cell and consists of square planar units of Pd atoms fourfold coordinated with oxygen atoms.²⁶ The bulk-terminated $\text{PdO}(101)$ surface is

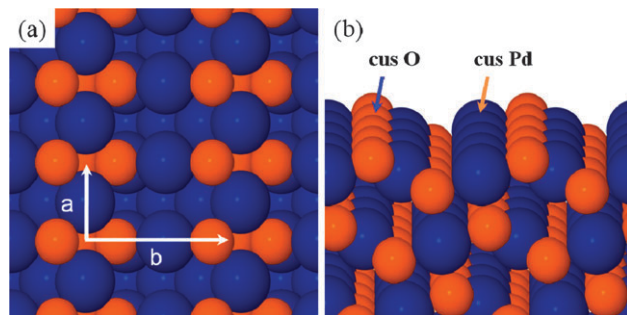


Fig. 2 Model representation of the stoichiometric $\text{PdO}(101)$ surface identifying coordinatively saturated (4f) and coordinatively unsaturated (cus) Pd and O atoms. The a and b directions correspond to the $[010]$ and $[\bar{1}01]$ crystallographic directions of PdO .

defined by a rectangular unit cell, where the a and b lattice vectors coincide with the $[010]$ and $[\bar{1}01]$ directions of the PdO crystal, respectively. The stoichiometric $\text{PdO}(101)$ surface consists of alternating rows of threefold or fourfold coordinated Pd or O atoms that run parallel to the a direction shown in Fig. 2. Thus, half of the surface O and Pd atoms are coordinatively unsaturated (cus). The side view of $\text{PdO}(101)$ shows that the coordinative environment associated with each cus-Pd atom resembles a square planar Pd complex with a coordination vacancy directed away from the surface and three oxygen ligands, one of which is a cus-O atom. The areal density of each type of coordinatively-distinct atom of the $\text{PdO}(101)$ surface is equal to 35% of the atomic density of the $\text{Pd}(111)$ surface. Hence, the coverage of cus-Pd atoms is equal to 0.35 ML (monolayer), and each $\text{PdO}(101)$ layer contains 0.7 ML of Pd atoms and 0.7 ML of O atoms, where we define 1 ML as equal to the surface atom density of $\text{Pd}(111)$. The presence of cus-Pd-O pairs is responsible for the high reactivity of the $\text{PdO}(101)$ surface toward alkanes.⁵

3.2. Facile C–H bond activation of propane on $\text{PdO}(101)$

The original discovery of strongly-bound molecular precursors and facile alkane dissociation on $\text{PdO}(101)$ was made through experiments of the adsorption and oxidation of propane on a $\text{PdO}(101)$ thin film that is grown on $\text{Pd}(111)$ in UHV.¹ Fig. 3 shows the results of temperature programmed reaction spectroscopy (TPRS) experiments performed after saturating the $\text{PdO}(101)$ surface with propane at 85 K. The data reveal that a fraction of the molecularly adsorbed propane desorbs without reacting, generating two main TPD features centered at 120 and 190 K. The remaining propane is completely oxidized by the surface during heating to produce H_2O and CO_2 which desorb simultaneously in reaction-limited peaks at ~ 465 K. A small fraction of H_2O also evolves in a desorption-limited peak near 350 K during the TPRS measurement.

The behavior observed during TPRS is consistent with a facile pathway for the precursor-mediated dissociation of propane on $\text{PdO}(101)$. In particular, the data show that a significant fraction of the molecularly adsorbed propane dissociates rather than desorbing during TPRS, and that the initial

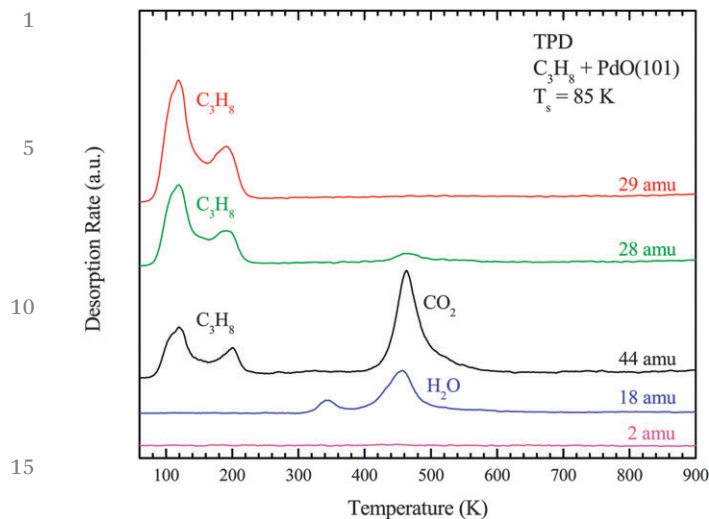


Fig. 3 TPRS spectra of m/z ratios equal to 29 (propane), 28 (propane + CO), 44 (propane + CO₂), 18 (H₂O) and 2 (H₂) obtained after saturating a PdO(101) surface with propane at 85 K. Reprinted with permission from ref. 1. Copyright 2009 American Chemical Society.

dissociation occurs before the molecularly-adsorbed propane desorbs from the surface at temperatures below about 200 K. The data further suggest that initial dissociation occurs by cleavage of a single C–H bond and that the resulting propyl fragments remain stable on the surface up to about 400 K. Support for this interpretation comes from the relative yields of the desorption and reaction-limited H₂O TPRS features. Analysis of the data shows that about seven times as much water desorbs in the reaction-limited peak compared with the desorption-limited peak, which implies that C₃H₈ dissociates below 200 K to liberate a H-atom which reacts with the surface to generate the H₂O peak at 350 K, and that the resulting C₃H₇ species undergoes negligible dehydrogenation until about 400 K, at which point this species is rapidly oxidized by the surface to generate the reaction-limited H₂O and CO₂ peaks at 465 K. The high reactivity of propane on PdO(101) represents the first example in which an alkane molecule was found to undergo facile dissociation on an oxide surface under UHV conditions. This observation suggests that the PdO(101) surface engages in a strong interaction with propane, the likes of which had not been identified for other oxides.

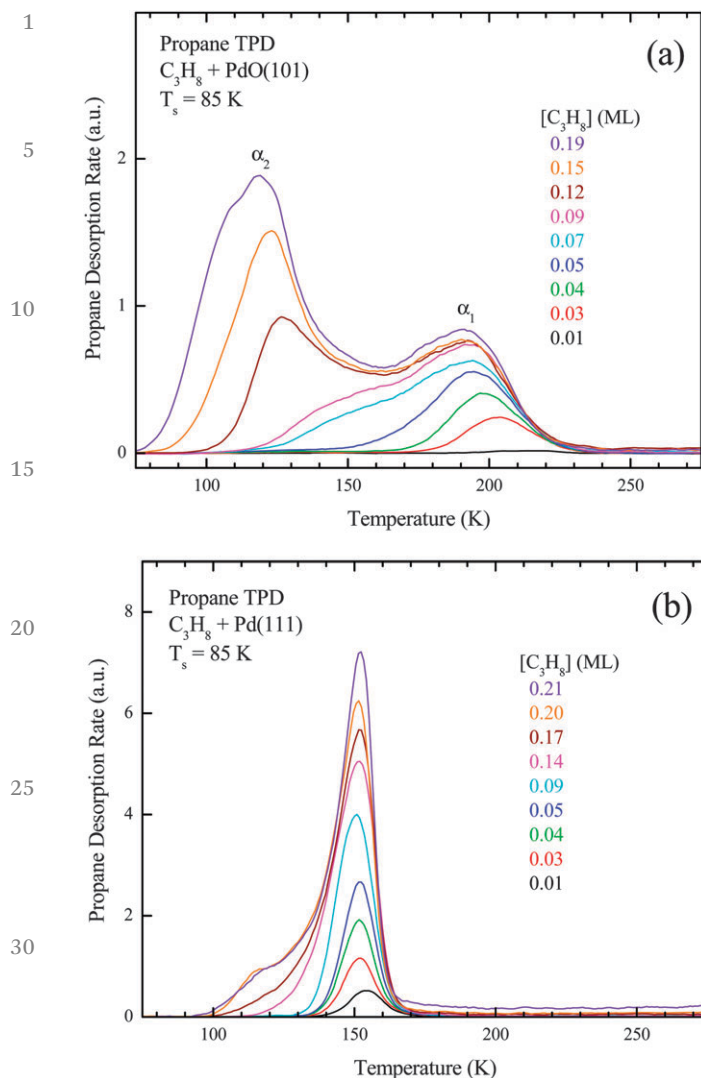
To test the idea that propane dissociates on PdO(101) from a molecularly-adsorbed state, Weaver *et al.*¹ performed measurements to estimate the initial dissociation probability S_0 of propane on PdO(101) as a function of the surface temperature T_s , where S_0 is defined as the dissociation probability in the limit of zero surface coverage of propane. In that work, the initial dissociation probability at a given temperature was estimated from TPRS measurements of the CO₂ desorption yields as a function of the propane exposure. These measurements show that the initial dissociation probability of propane on PdO(101) decreases with increasing surface temperature from 250 to 300 K, and thus that the apparent activation energy for propane dissociation is negative on the oxide surface. The

authors showed that a simple kinetic model for precursor-mediated C–H bond cleavage accurately reproduces the measured dependence of S_0 on T_s . The model assumes that a molecularly-adsorbed state of propane serves as the precursor for dissociation and that a kinetic competition between dissociation and desorption of the precursor determines the net dissociation probability. From the model, the initial dissociation probability is given by the equation $S_0 = \alpha k_r / (k_r + k_d)$ where α is the probability for molecular adsorption, and is close to unity for the conditions studied, and k_r and k_d represent rate coefficients for dissociation (“reaction”) and desorption, respectively. Analysis of the data using the precursor-mediated model gives values of $E_r - E_d = -16.2 \text{ kJ mol}^{-1}$ and $\nu_r/\nu_d = 3.9 \times 10^{-4}$ for the apparent activation energy and the apparent pre-factor for propane dissociation on PdO(101), respectively, and supports the conclusion that propane dissociation on PdO(101) occurs by a facile, precursor-mediated mechanism. Additional studies have provided insights into the nature of the molecular precursor and the reasons that this species readily dissociates on PdO(101).

3.3. Molecular precursors for propane dissociation on PdO(101)

A comparison of propane TPD spectra obtained from PdO(101) vs. Pd(111) indeed demonstrates that propane molecules bind strongly on the oxide surface. Fig. 4 shows propane TPD spectra obtained from PdO(101) and Pd(111) as a function of the initial propane coverage generated at 85 K. Propane physically adsorbs on Pd(111) and desorbs in a single TPD peak centered at 155 K, with a small amount of second layer propane desorbing in a shoulder at 120 K. Propane dissociates on Pd(111) to an immeasurable extent during the TPD experiments, in contrast to the significant reactivity that propane exhibits on the PdO(101) surface. The propane TPD spectra obtained from PdO(101) exhibit a broad desorption feature that consists of two distinct maxima centered at ~ 120 and 190 K, and denoted as the α_2 and α_1 states, respectively. The α_1 and α_2 desorption features develop nearly sequentially with increasing propane coverage, with propane initially populating the α_1 state. Since the oxide offers greater diversity in binding sites than Pd(111), it is not surprising that the propane desorption behavior is more complex for PdO(101). Interestingly, however, the total saturation coverage is approximately the same for the propane monolayers on PdO(101) and Pd(111), at a value of ~ 0.20 ML. Assuming that the propane which reacts, and desorbs as CO₂ and H₂O, originates from the α_1 state, one estimates that propane adsorbs in equal quantities in the α_1 and α_2 states when the propane monolayer on PdO(101) is saturated at 85 K. A likely interpretation is that the α_1 and α_2 states correspond to propane molecules adsorbed on the *cus* vs. *4f* Pd sites, respectively, since these sites are also present in equal concentrations on the PdO(101) surface.

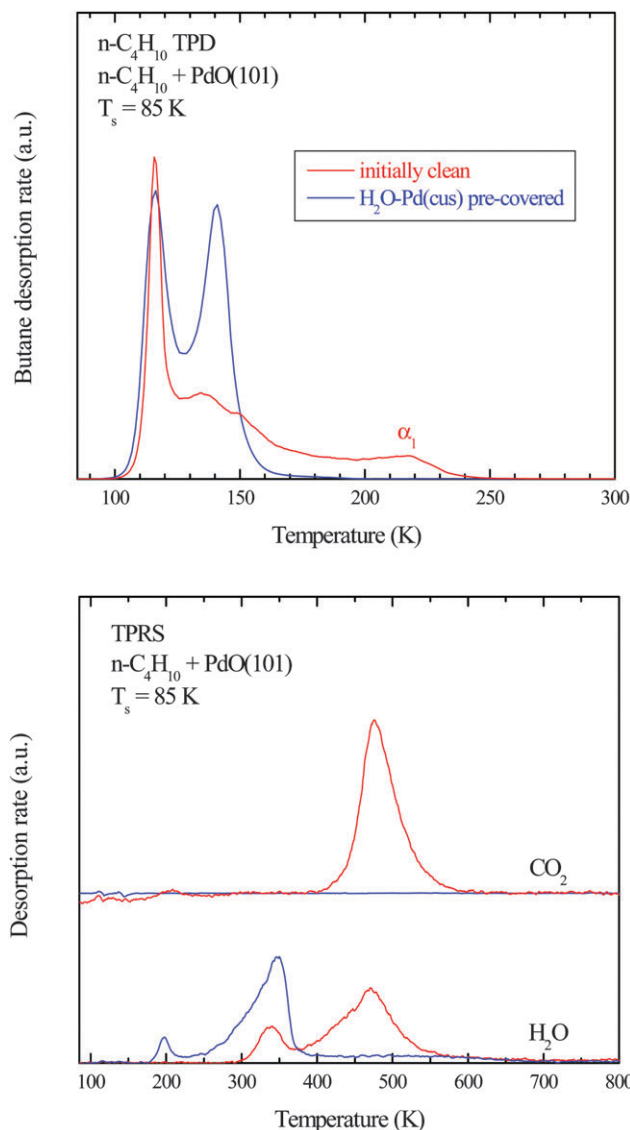
Significantly, the propane TPD data reveal that propane adsorbed in the α_1 state on PdO(101) has a higher binding energy than propane which is physically adsorbed on Pd(111). This result was rather surprising because, as mentioned above,



35 Fig. 4 Propane TPD spectra obtained from (a) PdO(101) and (b) Pd(111) as a function of the initial propane coverage prepared at 85 K. Reprinted with permission from ref. 1. Copyright 2009 American Chemical Society.

one generally expects higher binding energies when alkanes are physically adsorbed on a metal *vs.* a metal oxide, similar to the observations of Tait *et al.*¹⁹ for alkanes adsorbed on Pt(111) *vs.* MgO(100). The high binding energy associated with the α_1 state caused the authors to speculate that propane molecules experience a chemical bonding interaction in the α_1 state on PdO(101) that occurs negligibly on Pd(111) and enhances the α_1 propane binding energies on PdO(101) beyond that of physically adsorbed propane on Pd(111).¹

Experiments have established that the α_1 state of adsorbed propane and higher *n*-alkanes serves as the precursor for alkane C–H bond cleavage on the PdO(101) surface. For example, the yield of dissociated propane correlates with the amount of propane which desorbs in the α_1 state, but is independent of the coverage of propane in the more weakly-bound α_2 state.¹ Site blocking experiments provide particularly convincing evidence that the α_1 state serves as the precursor for alkane dissociation on PdO(101) and that the precursor binds to the



35 Fig. 5 TPRS spectra of *n*-butane (top) and CO₂ and H₂O (bottom) obtained after adsorbing *n*-butane on clean PdO(101) (red curves) *vs.* a H₂O-precovered PdO(101) surface (blue curves). Water was adsorbed on PdO(101) at 250 K to selectively bind water only on the Pd_{cus} sites. Reprinted with permission from ref. 27. Copyright 2013 Elsevier.

cus-Pd sites of the surface.^{2,27} Fig. 5 shows *n*-butane, CO₂ and H₂O TPRS traces obtained after adsorbing *n*-butane onto clean *vs.* H₂O pre-covered PdO(101).²⁷ In these experiments, the water layer was prepared at 250 K to selectively saturate the cus-Pd sites with H₂O while avoiding water adsorption onto the 4f-Pd sites.²⁸ The TPRS results demonstrate that the pre-adsorbed water completely suppresses both the adsorption of *n*-butane into the strongly-bound α_1 state and the initial dissociation of *n*-butane, where the latter is evidenced by a lack of reaction-limited CO₂ and H₂O desorption. These results reveal that the *n*-butane molecules must adsorb into the α_1 state to undergo C–H bond cleavage during TPRS, and further show that the α_1 state arises from *n*-butane molecules that are associated with the cus-Pd sites of the PdO(101) surface.

3.4. Adsorbed alkane σ -complexes on PdO(101)

The binding of n -alkanes adsorbed in the strongly-bound α_1 state on PdO(101) has been investigated extensively both experimentally and computationally. Fig. 6 shows a plot of molecular binding energies as a function of the chain length for n -alkanes (C_1 to C_5) adsorbed on both Pd(111) and in the α_1 state on PdO(101), where the binding energies were determined from an analysis of experimental TPD data.^{2,29} It is important to mention that neither methane nor ethane measurably dissociate on PdO(101) during TPD experiments in UHV, but that the C_3 to C_5 n -alkanes dissociate readily during TPD. Recent dispersion-corrected DFT calculations reproduce these trends in n -alkane reactivity on PdO(101).³⁰ The plot in Fig. 6 shows that the binding energies are enhanced by a nearly constant amount for n -alkanes adsorbed on PdO(101) vs. Pd(111), and that the E_d vs. N relation for PdO(101) is linear but exhibits an intercept on the y -axis that is significantly larger than zero (~ 25 kJ mol⁻¹). Indeed, this comparison demonstrates that the enhanced binding on PdO(101) relative to Pd(111) is a common feature in the binding of n -alkanes on the oxide surface.

The authors suggested that two main energetic contributions can explain the nature of the E_d vs. N relation for n -alkanes adsorbed on PdO(101). The linear increase was attributed to a chain-length dependent contribution that arises from molecule-surface dispersion interactions, which is analogous to the explanation given previously of the linear E_d vs. N relations for n -alkanes that are physically adsorbed on close-packed surfaces.¹⁹ The non-zero intercept was attributed to dative bonding interactions between the alkanes and the cus-Pd atoms of the PdO(101) surface, which enhance the alkane-surface binding on PdO(101) beyond that afforded by only dispersion interactions. The constant enhancement suggests that the molecule-surface dative bonding produces a similar contribution to the total binding energy for the n -alkanes studied (C_1 to C_5).

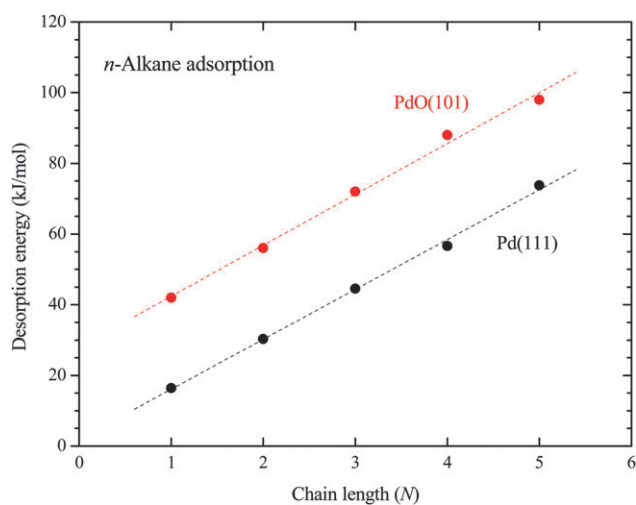


Fig. 6 Desorption energy as a function of the molecular chain length for n -alkanes adsorbed on PdO(101) and Pd(111). The desorption activation energies were estimated from TPD data and the energies reported for PdO(101) correspond to alkanes adsorbed as σ -complexes (α_1 TPD peak).

DFT calculations support the interpretation that n -alkanes datively bond with the cus-Pd atoms of PdO(101), resulting in adsorbed alkane σ -complexes.^{2,5,9,29-33} In general, a dative (or coordinate) bond is a covalent bond in which the shared electrons originate from only one species that is involved in the bonding. In an alkane σ -complex, one or more C-H bonds of the alkane acts as a ligand and donates electrons into empty d-states of the transition metal atom.¹⁰ Back-donation of charge from filled d-states into unoccupied molecular orbitals of the alkane can also contribute to the bonding in an alkane σ -complex. According to DFT, CH_4 adopts an η^2 configuration on PdO(101) in which the CH_4 molecule straddles a cus-Pd atom and places the two Pd-coordinated C-H bonds in a plane that is parallel to the cus-Pd row.^{2,29,30,32} DFT also predicts that CH_4 binds more strongly on PdO(101) than Pd(111), with binding energies of about 16 and 2 kJ mol⁻¹, respectively.²⁹ Since conventional DFT accounts for bonding interactions, but does not describe dispersion interactions, the calculations suggest that CH_4 experiences a form of covalent bonding with the cus-Pd atoms of PdO(101) and that such an interaction occurs to a negligible extent on the Pd(111) surface.

DFT-derived changes in the charge distribution and electronic structure that are induced by CH_4 adsorption on PdO(101) demonstrate that the methane molecule experiences a donor-acceptor interaction with the cus-Pd atom. Fig. 7 shows a charge-density difference plot that is obtained by subtracting the charge distribution of the isolated CH_4 molecule plus the clean PdO(101) surface from that predicted for the η^2 CH_4 complex on PdO(101).²⁹ The plot reveals that electrons accumulate between the CH_4 molecule and the cus-Pd atom and that the electron density is depleted near the cus-Pd atom. The latter feature is characteristic of back-bonding in which electrons from filled d-states of the cus-Pd atom occupy anti-bonding orbitals of the CH_4 molecule that are empty when the molecule is isolated from the surface. Such back-donation of charge is expected to strengthen the molecule-surface

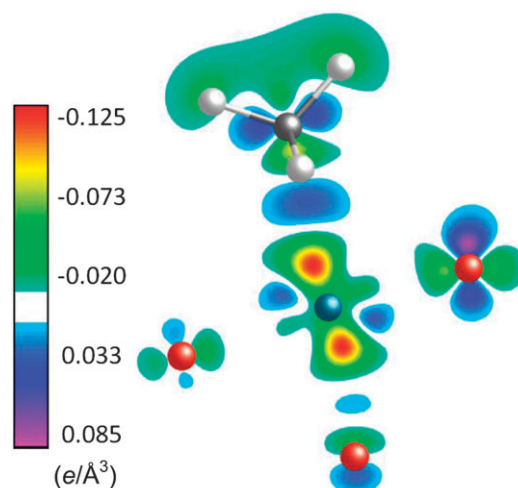


Fig. 7 Difference charge density plot determined by DFT for the CH_4 $\eta^2(H, H)$ complex adsorbed on a Pd_{cus} site of PdO(101). Reprinted with permission from ref. 29. Copyright 2010 American Institute of Physics.

1 binding while weakening intramolecular bonds of the adsorbed
species. Consistent with this idea, normal mode analysis pre-
dicts that vibrational modes which involve motions of the Pd-
coordinated C–H bonds are redshifted by as much as 200 cm^{-1}
5 from their gas-phase values, thus confirming that the dative
bonding interaction with the surface softens C–H bonds.²

To investigate the role of alkane–surface dative bonding in
promoting C–H bond cleavage on PdO(101), Weaver *et al.*²
calculated energy barriers for the cleavage of a Pd-
coordinated C–H bond *vs.* a “non-activated” C–H bond of the
10 CH₄ η^2 complex, where the latter bond corresponds to one of
the C–H bonds that is directed away from the surface and is not
directly involved in the dative interaction. These calculations
predict that the energy barrier for breaking one of the Pd-
coordinated C–H bonds is lower by more than 100 kJ mol^{-1}
15 than the barrier for breaking a non-activated C–H bond of the
CH₄ complex on PdO(101), demonstrating that the dative
bonding interaction significantly weakens alkane C–H bonds.
Using DFT, Hellman *et al.*⁹ have further shown that the
20 population of filled 5s states is low on the cus-Pd atoms of
PdO(101) and consequently promotes a bonding interaction
with the CH₄ molecule in addition to reducing the C–H bond
cleavage barrier. In contrast, the electron density in the 5s state
is higher for surface Pd atoms of bulk PdO(100) as well as a
25 monolayer PdO(101) film on Pd(100), and the CH₄ molecule
consequently experiences a repulsive interaction with these Pd
oxide surfaces and larger dissociation barriers.

Overall, prior studies demonstrate that the formation of
adsorbed alkane σ -complexes is critical to achieving facile C–
H bond cleavage on the PdO(101) surface. In the context of the
potential energy diagram of Fig. 1, the formation of an
adsorbed σ -complex enhances alkane binding to the surface
relative to that achieved by physisorption alone, and thereby
increases the desorption activation energy E_d . In addition, σ -
35 complex formation weakens the Pd-coordinated C–H bonds
and thus acts to lower the intrinsic activation energy for
reaction E_r . Both of these effects serve to lower the apparent
energy barrier ($E_r - E_d$) for alkane C–H bond cleavage on
PdO(101), making PdO(101) highly reactive toward alkane dis-
40 sociation. As discussed below, DFT calculations also predict the
formation and facile C–H bond activation of alkane σ -
complexes on RuO₂ and IrO₂ surfaces. An implication is that
a high activity toward alkane dissociation is not limited to the
PdO(101) surface, but is a property of other late transition-
45 metal oxide surfaces as well.

3.5. Binding energies and configurations of *n*-alkanes on PdO(101)

Accurately predicting the binding energies of alkanes on solid
surfaces is essential for developing kinetic models of alkane
surface chemistry and requires an accurate treatment of mole-
cule–surface dispersion interactions. Antony *et al.*³⁰ have
recently shown that a dispersion-corrected DFT method (DFT-
D3) significantly improves the accuracy of binding energies
55 computed for *n*-alkanes adsorbed on the Pd(111) and PdO(101)
surfaces. The DFT-D3 method, developed by Grimme and

coworkers,³⁴ combines conventional DFT with a semi-
empirical calculation of the dispersion energy in a molecular
system where the dispersion energy is computed after the self-
consistent determination of the electronic energy. The results
of Antony *et al.*³⁰ show that conventional DFT significantly
5 underestimates alkane binding energies on the Pd surfaces,
as expected, and that the DFT-D3 method brings the binding
energies into close agreement with measured values. On
PdO(101), the binding energies predicted by DFT-D3 agree to
within about 5% of experimental values for the C₁ to
10 C₄ *n*-alkanes; with increasing chain length to C₄, the predicted
n-alkane binding energies on PdO(101) are about 41, 57, 72 and
86 kJ mol^{-1} . According to the calculations, dispersion interac-
tions account for about 65% of the binding energies of alkane
 σ -complexes on PdO(101) with dative bonding and electrostatic
15 interactions contributing the remaining 35%. In contrast, DFT-
D3 predicts that dispersion interactions are almost entirely
responsible for the molecular binding of alkanes on the
close-packed Pd(111) surface.

The DFT-D3 calculations of Antony *et al.*³⁰ predict that, in
20 general, *n*-alkanes can adopt multiple stable configurations on
PdO(101), but follow a trend in which the preferred configu-
ration changes with increasing molecular chain length. Accord-
ing to the calculations, methane and ethane preferentially bind
in η^2 configurations in which a H–C–H bond angle straddles a
25 cus-Pd atom (*e.g.*, Fig. 7). For larger *n*-alkanes, steric repulsion
with the cus-O atom row destabilizes η^2 configurations and
causes the *n*-alkane molecules to preferentially align along the
cus-Pd row and adopt η^1 configurations in which single H–Pd
dative bonds form at different CH_{*n*} groups along the molecular
30 chain. Propane represents a special case since an η^2 configu-
ration is nearly energetically degenerate to an η^1 configu-
ration.^{30,31} The *n*-alkanes larger than propane strongly prefer
to adsorb on PdO(101) in all-trans conformations and adopt η^1
35 bonding configurations along the cus-Pd row.

3.6. Kinetics of alkane dissociation on PdO(101)

Antony *et al.*³¹ have recently reported a microkinetic model that
accurately reproduces the initial dissociation probability of
propane on PdO(101) as a function of the surface temperature
40 as well as the measured kinetic parameters. The microkinetic
model utilizes formulas from transition state theory (TST) to
compute rate coefficients, with binding energies, energy bar-
riers for C–H bond cleavage and vibrational properties deter-
mined from the results of DFT-D3 calculations. The model also
45 takes into account the possibility that propane can adsorb on
PdO(101) in different molecular configurations. From TST, the
rate coefficient for the reaction of an adsorbed species is given
by an equation of the general form,

$$k = \frac{k_B T}{h} \frac{q^\ddagger}{q_{\text{ad}}} \exp\left(-\frac{\Delta E^\ddagger}{k_B T}\right)$$

where ΔE^\ddagger represents the zero-point corrected energy barrier
50 for reaction and q^\ddagger and q_{ad} represent partition functions for the
transition state and the initial adsorbed state, respectively. The

ratio $q^{\ddagger}/q_{\text{ad}}$ is proportional to the entropy difference between the transition state and the initial state. Accurately describing the partition functions and hence entropies of the adsorbed alkanes is challenging because the frustrated translations and rotations of these species are only weakly hindered and thus behave in a manner that is intermediate to free motions and localized vibrations.

Antony *et al.*³¹ compared two approaches for calculating the partition functions of the adsorbed alkane structures, designated as the $3N$ and $3N - 2$ models. In the $3N$ model, all motions of the adsorbed alkanes and the transition states (TS) for C–H bond cleavage are modeled as harmonic oscillators and the partition functions are computed using the formula for $3N$ uncoupled harmonic oscillators. In the $3N - 2$ model, two of the frustrated motions (one translation and one rotation) are modeled as free motions while the remaining motions are treated as harmonic oscillators. Fig. 8 shows the initial dissociation probability of propane on PdO(101) as a function of the surface temperature computed using the $3N$ and $3N - 2$ models as well as that determined experimentally. As seen in the figure, the $3N$ model underestimates the measured S_0 values by two to three orders of magnitude over the temperature range studied, whereas the $3N - 2$ model predicts S_0 values that agree to within better than 25% of the measured values. The $3N$ and $3N - 2$ models predict apparent activation energies for dissociation of $E_r - E_d = -18.1$ and -18.4 kJ mol⁻¹, respectively, which agree to within better than 14% of the experimental estimate of -16.2 kJ mol⁻¹. The good agreement between the predicted and experimental activation energies is encouraging as it suggests the possibility that the DFT-D3 method can provide chemical accuracy in predicting alkane C–H bond cleavage barriers. In contrast, however, the $3N$ model

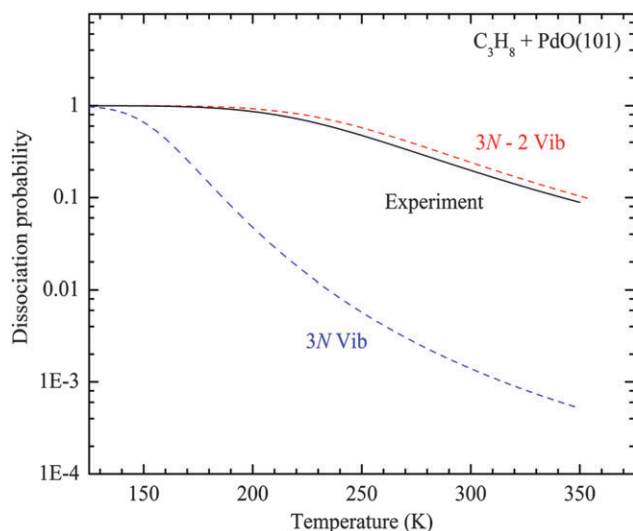


Fig. 8 Initial dissociation probability of propane on PdO(101) as a function of the surface temperature as determined experimentally and using the $3N$ and $3N - 2$ microkinetic models discussed in the text. The microkinetic models employ parameters derived from DFT-D3 calculations. Reprinted with permission from ref. 31. Copyright 2012 Royal Society of Chemistry.

predicts an apparent pre-factor for dissociation ν_r/ν_d that is about a factor of 200 lower than the experimental value (10^{-6} vs. 3.9×10^{-4}), whereas the $3N - 2$ model predicts $\nu_r/\nu_d = 2.0 \times 10^{-4}$, which is within a factor of two of the experimental estimate. The $3N$ model also predicts apparent pre-factors for the dissociation of methane and ethane on PdO(101) that are 10 to 50 times lower than the values predicted by the $3N - 2$ model.³² It is worth noting that the microkinetic models predict that neither methane nor ethane should measurably dissociate on PdO(101) during TPD experiments, which is consistent with experimental observations.^{29,32}

The studies of Antony *et al.*^{31,32} highlight the importance of accurately describing entropic contributions in kinetic models of alkane dissociation on surfaces. Key findings are that adsorbed alkanes have significantly higher entropies than are predicted by harmonic TST at temperatures where dissociation and desorption rates are appreciable, and that the $3N - 2$ model, in which two of the frustrated adsorbate motions are treated as free motions, provides accurate estimates of the entropies of adsorbed propane species on PdO(101). Significantly, recent work by Campbell and Sellers shows that the entropies of many adsorbed molecules are considerably higher than the predictions of harmonic TST at temperatures for appreciable desorption rates.^{35,36} Those authors show that the entropies of many adsorbed species, including alkanes, are equal to about 70% of the entropies of the corresponding gas-phase molecules and that these entropies are linearly correlated. The large slope of the Campbell-Sellers correlation suggests that many adsorbed molecules move nearly freely within the plane of a solid surface near the onset for desorption, though the molecule-surface interaction does continue to slightly restrict the in-plane motion.³⁷ Indeed, this finding further demonstrates the need to develop accurate methods for describing the entropies of adsorbed species when modeling surface reaction kinetics. Such methods will ultimately need to take into account more explicit details of the weakly-hindered motions that molecules execute within the surface plane, and consider key features of the molecule-surface potential energy surface. Overall, the work of Antony *et al.*^{31,32} reveals the possibility of accurately predicting alkane dissociation rates on solid surfaces using microkinetic modeling. Stringent comparisons with experimental data are needed to assess the accuracy of both the energetic and entropic contributions that are estimated from DFT-D3 and the $3N - 2$ model.

4. Methane C–H bond activation on RuO₂ and IrO₂ surfaces

Recent results suggest that the formation and facile C–H bond activation of alkane σ -complexes is not limited to the PdO(101) surface, but also occurs on RuO₂ and IrO₂ surfaces. For example, an experimental study by Erlekam *et al.*³⁸ shows that methane and ethane adsorb strongly on RuO₂(110) and achieve binding energies that are similar to alkane σ -complexes on

PdO(101). As with PdO(101), neither methane nor ethane measurably dissociates on RuO₂(110) during TPD experiments. Recently, Wang *et al.*³⁹ have reported DFT results which predict that methane binds strongly on the IrO₂(110) surface and that the energy barrier for C–H bond cleavage is lower than that for desorption of the molecularly adsorbed species by more than ~20 kJ mol⁻¹. Similar to findings for methane on PdO(101), DFT predicts that CH₄ forms a strongly-bound σ -complex on IrO₂(110) by datively bonding with an Ir_{cus} atom. Indeed, a common feature of the PdO(101), RuO₂(110) and IrO₂(110) surfaces is that they each expose rows of coordinatively-unsaturated metal and oxygen atoms that interact strongly with adsorbed alkanes.

Motivated by these findings, our groups have recently examined CH₄ adsorption and activation on RuO₂ and IrO₂ surfaces using DFT-D3 calculations. Fig. 9 shows energy diagrams summarizing pathways for C–H bond activation of CH₄ σ -complexes on PdO(101), RuO₂(110) and IrO₂(100) surfaces as computed using DFT-D3. The energies of each stationary state are corrected for zero-point vibrational energy. The plots reveal that CH₄ binds strongly on each of the oxide surfaces considered, achieving binding energies between about 37 and 50 kJ mol⁻¹, and that the barriers for C–H bond cleavage are also very similar (~56 kJ mol⁻¹) among these surfaces. As expected, analysis of the electronic structures and charge density differences reveals that the strongly-bound molecular states of methane on RuO₂(110) and IrO₂(100) may be regarded as σ -complexes. Notice that the apparent energy barriers for CH₄ dissociation ($E_r - E_d$) vary from about 6 to 19 kJ mol⁻¹ on the oxide surfaces considered in our calculations. These barriers are comparable to or lower than apparent activation energies that have been reported for methane dissociation on the most reactive transition-metal surfaces that have been investigated in detail.^{14,40–44}

The few studies reported to date reveal that RuO₂ and IrO₂ surfaces exhibit similar behavior as PdO(101) toward binding and activating small alkanes. Since the high activity of these materials toward alkane activation arises from the presence of

cus-metal and oxygen surface sites, it is reasonable to anticipate that other late transition-metal oxide surfaces will also be reactive toward alkanes as long as cus-surface sites are available. Excluding the study by Erlekam *et al.*,³⁸ experimental investigations of alkane adsorption and activation on late transition-metal oxide surfaces other than PdO(101) have not yet been reported, which suggests that this class of surface chemical interactions is fertile ground for future investigation. In general, a key challenge for such studies is the development of methods for generating well-defined oxide surfaces for model UHV experiments.

Among the late transition-metal oxides, RuO₂(110) and PdO(101) surfaces can be routinely prepared as high-quality thin films under UHV conditions. Recent work also demonstrates that IrO₂(100) domains form during the oxidation of Ir(111) by O-atom beams,⁴⁵ but the structural properties of these surfaces have not yet been examined in detail. While procedures for growing high-quality PdO(101) thin films involve the use of O-atom beams to oxidize Pd(111), methods for growing RuO₂(110) films are more accessible since they involve the oxidation of Ru(0001) using O₂ under vacuum conditions.⁴⁶ As mentioned, the adsorption behavior of CH₄ and C₂H₆ is similar on the RuO₂(110) and PdO(101) surfaces – both molecules adsorb as σ -complexes but do not react during TPD experiments because the apparent activation energies for dissociation are positive for both surfaces (Fig. 9). Using DFT-D3, Antony has recently predicted that $E_r - E_d$ is negative for propane dissociation on RuO₂(110), and has a value that is similar to that determined for the propane–PdO(101) system. One can thus expect that propane and larger *n*-alkanes will readily dissociate on the RuO₂(110) surface under UHV conditions. Overall, recent studies suggest that several late transition-metal oxide surfaces will exhibit high reactivity toward alkanes due to the availability of both cus-metal and oxygen surface sites. Experimental investigations with different late transition-metal oxide surfaces can thus help to further clarify the specific properties of these materials which promote alkane σ -complex formation and C–H bond activation, and

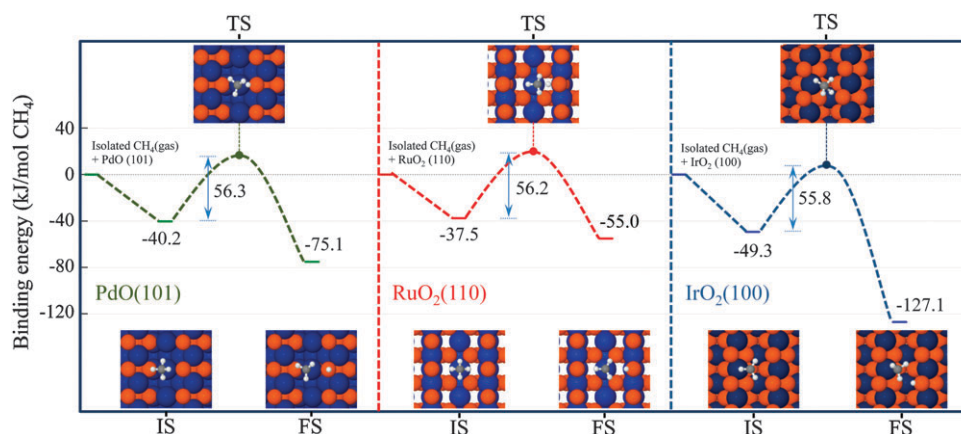


Fig. 9 Energy pathways and molecular configurations for C–H bond cleavage of CH₄ η^2 complexes adsorbed on PdO(101), RuO₂(110) and IrO₂(100) as determined by the DFT-D3 method. Energies are shown in units of kJ mol⁻¹.

ultimately facilitate the design of oxides that exhibit high activity and selectivity toward the oxidation of alkanes.

5. Summary

Alkane activation on oxide surfaces plays a central role in many applications of oxidation catalysis, including the complete oxidation of alkanes for applications in power generation and pollution control as well as the selective oxidation of alkanes to value-added products. Advances in the fundamental understanding of alkane activation on oxide surfaces have strong potential for guiding the design of new catalytic processes that efficiently utilize alkanes as well as improving existing applications. Although model investigations of alkane chemistry on crystalline oxide surfaces are limited, detailed studies of alkane adsorption and activation on the PdO(101) surface provide insights that may be broadly applicable for understanding the interactions of alkanes with oxides of the late transition metals.

This review summarizes recent findings of our investigations of alkane activation on the PdO(101) surface as well as results of investigations of methane activation on IrO₂ and RuO₂ surfaces. These studies demonstrate that alkanes form strongly-bound σ -complexes on the PdO(101) surface by datively bonding with *cus*-Pd atoms at the surface, and that the σ -complexes serve as precursors for C–H bond activation. Our studies reveal that the alkane–surface dative interactions enhance the binding of the adsorbed σ -complexes beyond that afforded by dispersion interactions alone, and also weaken the Pd-coordinated C–H bonds. Both of these effects serve to lower the apparent activation energy ($E_r - E_d$) for dissociative chemisorption, and thus increase alkane dissociation probabilities significantly. Experiments reveal that propane and larger *n*-alkanes dissociate on PdO(101) at temperatures below about 215 K during UHV experiments. Computations using the dispersion-corrected DFT-D3 method provide very good agreement with experimental estimates of *n*-alkane binding energies on PdO(101), and provide insights into the preferred binding configurations of the *n*-alkane σ -complexes. We also discuss recent work showing that a microkinetic model, parameterized using results of DFT-D3 calculations, accurately reproduces measured dissociation rates of propane on PdO(101) as a function of the surface temperature. The kinetic modeling studies highlight the importance of entropic contributions in alkane dissociation on solid surfaces. Lastly, we report DFT calculations which predict that the formation and facile C–H bond activation of alkane σ -complexes is not limited to PdO(101) but occurs on RuO₂ and IrO₂ surfaces as well. This finding suggests that many late transition metal oxide surfaces interact strongly with alkanes, and thus represent a promising class of materials from which to base the design of new catalysts for effecting chemical transformations of alkanes.

Acknowledgements

We acknowledge the Ohio Supercomputing Center for providing computational resources. We also gratefully acknowledge

financial support for this work provided by the U.S. Department of Energy, Office of Basic Energy Sciences, Catalysis Science Division through Grant DE-FG02-03ER15478.

References

- 1 J. F. Weaver, S. P. Devarajan and C. Hakanoglu, *J. Phys. Chem. C*, 2009, **113**, 9773.
- 2 J. F. Weaver, J. A. Hinojosa, C. Hakanoglu, A. Antony, J. M. Hawkins and A. Asthagiri, *Catal. Today*, 2011, **160**, 213.
- 3 J. F. Weaver, C. Hakanoglu, A. Antony and A. Asthagiri, *J. Am. Chem. Soc.*, 2011, **133**, 16196.
- 4 C. Hakanoglu, F. Zhang, A. Antony, A. Asthagiri and J. F. Weaver, *Phys. Chem. Chem. Phys.*, 2013, **15**, 12075.
- 5 J. F. Weaver, *Chem. Rev.*, 2013, **113**, 4164–4215.
- 6 J. G. McCarty, *Catal. Today*, 1995, **26**, 283.
- 7 R. van Rijn, O. Balmes, A. Resta, D. Wermeille, R. Westerstrom, J. Gustafson, R. Felici, E. Lundgren and J. W. M. Frenken, *Phys. Chem. Chem. Phys.*, 2011, **13**, 13167.
- 8 R. Westerstrom, M. E. Messing, S. Blomberg, A. Hellman, H. Gronbeck, J. Gustafson, N. M. Martin, O. Balmes, R. van Rijn, J. N. Andersen, K. Deppert, H. Bluhm, Z. Liu, M. E. Grass, M. Havecker and E. Lundgren, *Phys. Rev. B: Condens. Matter Mater. Phys.*, 2011, **83**, 115440.
- 9 A. Hellman, A. Resta, N. M. Martin, J. Gustafson, A. Trincherro, P. A. Carlsson, O. Balmes, R. Felici, R. van Rijn, J. W. M. Frenken, J. N. Andersen, E. Lundgren and H. Gronbeck, *J. Phys. Chem. Lett.*, 2012, **3**, 678.
- 10 C. Hall and R. N. Perutz, *Chem. Rev.*, 1996, **96**, 3125.
- 11 R. H. Crabtree, *Angew. Chem., Int. Ed. Engl.*, 1993, **32**, 789.
- 12 R. H. Crabtree, *Chem. Rev.*, 1995, **95**, 987.
- 13 J. E. Bercaw and J. A. Labinger, *Proc. Natl. Acad. Sci. U. S. A.*, 2007, **104**, 6899.
- 14 J. F. Weaver, A. F. Carlsson and R. J. Madix, *Surf. Sci. Rep.*, 2003, **50**, 107.
- 15 S. L. Tait, Z. Dohnalek, C. T. Campbell and B. D. Kay, *J. Chem. Phys.*, 2005, **122**, 164707.
- 16 S. L. Tait, Z. Dohnalek, C. T. Campbell and B. D. Kay, *J. Chem. Phys.*, 2005, **122**, 164708.
- 17 M. D. Krcha, A. D. Mayernick and M. J. Janik, *J. Catal.*, 2012, **293**, 103.
- 18 E. W. McFarland and H. Metiu, *Chem. Rev.*, 2013, **113**, 4391.
- 19 S. L. Tait, Z. Dohnalek, C. T. Campbell and B. D. Kay, *J. Chem. Phys.*, 2006, **125**, 234308.
- 20 R. M. Slayton, C. M. Aubuchon, T. L. Camis, A. R. Noble and N. J. Tro, *J. Phys. Chem.*, 1995, **99**, 2151.
- 21 A. Chakradhar, Y. Liu, J. Schmidt, E. Kadossov and U. Burghaus, *Surf. Sci.*, 2011, **605**, 1537.
- 22 H. H. Kan, R. B. Shumbera and J. F. Weaver, *Surf. Sci.*, 2008, **602**, 1337.
- 23 H. H. Kan and J. F. Weaver, *Surf. Sci.*, 2008, **602**, L53.
- 24 H. H. Kan and J. F. Weaver, *Surf. Sci.*, 2009, **603**, 2671.
- 25 J. A. Hinojosa and J. F. Weaver, *Surf. Sci.*, 2011, **605**, 1797.
- 26 J. Rogal, K. Reuter and M. Scheffler, *Phys. Rev. B: Condens. Matter Mater. Phys.*, 2004, **69**, 075421.

- 1 27 F. Zhang, C. Hakanoglu, J. A. Hinojosa and J. F. Weaver, *Surf. Sci.*, 2013, **617**, 249.
- 28 H. H. Kan, R. J. Colmyer, A. Asthagiri and J. F. Weaver, *J. Phys. Chem. C*, 2009, **113**, 1495.
- 5 29 J. F. Weaver, C. Hakanoglu, J. M. Hawkins and A. Asthagiri, *J. Chem. Phys.*, 2010, **132**, 024709.
- 30 A. Antony, C. Hakanoglu, A. Asthagiri and J. F. Weaver, *J. Chem. Phys.*, 2012, **136**, 054702.
- 31 A. Antony, A. Asthagiri and J. F. Weaver, *Phys. Chem. Chem. Phys.*, 2012, **14**, 12202.
- 10 32 A. Antony, A. Asthagiri and J. F. Weaver, *J. Chem. Phys.*, 2013, **139**, 104702.
- 33 N. M. Kinnunen, J. T. Hirvi, M. Suvanto and T. A. Pakkanen, *J. Phys. Chem. C*, 2011, **115**, 19197.
- 15 34 S. Grimme, J. Antony, S. Ehrlich and H. Krieg, *J. Chem. Phys.*, 2010, **132**, 154104.
- 35 C. T. Campbell and J. R. V. Sellers, *J. Am. Chem. Soc.*, 2012, **134**, 18109.
- 36 C. T. Campbell and J. R. V. Sellers, *Chem. Rev.*, 2013, **113**, 4106.
- 37 J. F. Weaver, *Science*, 2013, **339**, 39.
- 38 U. Erlekam, U. A. Paulus, Y. Wang, H. P. Bonzel, K. Jacobi and G. Ertl, *Z. Phys. Chem.*, 2005, **219**, 891.
- 5 39 C. C. Wang, S. S. Siao and J. C. Jiang, *J. Phys. Chem. C*, 2012, **116**, 6367.
- 40 S. A. Soulen and R. J. Madix, *Surf. Sci.*, 1995, **323**, 1.
- 41 C. B. Mullins and W. H. Weinberg, *J. Chem. Phys.*, 1990, **92**, 4508.
- 42 C. T. Reeves, D. C. Seets and C. B. Mullins, *J. Mol. Catal. A: Chem.*, 2001, **167**, 207.
- 10 43 D. C. Seets, C. T. Reeves, B. A. Ferguson, M. C. Wheeler and C. B. Mullins, *J. Chem. Phys.*, 1997, **107**, 10229.
- 44 A. V. Hamza, H. P. Steinruck and R. J. Madix, *J. Chem. Phys.*, 1987, **86**, 6506.
- 15 45 W. H. Chung, D. S. Tsai, L. J. Fan, Y. W. Yang and Y. S. Huang, *Surf. Sci.*, 2012, **606**, 1965.
- 46 H. Over, *Chem. Rev.*, 2012, **112**, 3356.
- 20
- 25
- 30
- 35
- 40
- 45
- 50
- 55